CHAPTER 6 "EXPERIMENTAL EVIDENCE OF THE EFFECT OF ANISOTROPIC ROTATION ON NOE INTENSITIES"

6.1 Summary

This chapter addresses the issue of the effect of anisotropic molecular rotation on the nuclear Overhauser effect (NOE) as measured by NMR.

Three samples were examined. The first sample is nearly spherical in its hydrodynamic dimensions and the NOEs reflect this, they show no influence from anisotropic rotation. The second sample is cylindrical in shape with a long to short axis ratio of 2:1. The NOEs from this sample have been influenced by the rotational anisotropy due to the cylindrical shape. The third sample is also cylindrical in shape with a long to short axis ratio of 4:1, and it is with this sample that the strongest influence of the rotational anisotropy on the NOEs are seen.

6.2 Introduction

Methods for structure determination of biomolecules by NMR have historically relied heavily on the use of two primary experiments. The first is the Correlation Spectroscopy (COSY) experiment, and its many derivatives, which gives information relating the energy coupling of spin pairs which are connected via covalent bonds. Most notably, the 3 bond J (or scalar) coupling between two protons is important because the intensity of the coupling relates to the torsion angle formed between the protons. This can be exploited to determine the torsion angle. The most obvious limitation of using COSY data in structure determination is that the information corresponds only to short distances, the torsion angle can only lock down the geometry of a few atoms connected through-bond, which will be necessarily spatially close to one another.

The second major experiment used by NMR spectroscopists for structure determination is to measure the nuclear Overhauser effect. The NOE is a dipole-dipole relaxation rate process in which two magnetic nuclei are coupled by their dipole moments. The intensity of the measured NOE is dependent on the distance separation between the nuclei and is realized experimentally as a crosspeak in a two-dimensional NOESY experiment correlated to the frequencies of the two resonances. NOE information can be a powerful tool for structure elucidation in that it can relate the distances of covalently remote atoms, unlike the COSY data. This is especially important and useful for large biomolecules which may be folded into interesting secondary and tertiary structures.

In practice, however, the crosspeak intensity between two resonances of a NOESY experiment alone does not give the distance between the two nuclei. The NOE is a consequence of dipolar relaxation, and as such, it involves a number of complex processes, all of which must be understood in order to interpret the data correctly. Nuclear spin relaxation derives from the fluctuating magnetic fields surrounding a nucleus. These fields can come from a number of sources, molecular rotational diffusion, global molecular dynamics, localized atomic libration and others. To fully understand the NOE data, an accurate (and verifiable) model of all these motions is necessary. It is the inherent complexity of the underlying theory that has led to assumptions that simplify the interpretation of NOE data.

This chapter attempts to separate the effect of the molecular tumbling component of dipolar relaxation from those of structure and intramolecular dynamics. To do this, the samples chosen for study must meet two criteria: first, the samples must be composed of

(or contain a region of) fairly uninteresting "regular" structure; second, the samples must span a range of rotational motions, from spherical isotropic motion to cylindrical anisotropic motion. The first requirement is necessary because we will have to make assumptions about the structure and dynamics of the samples and we feel more confident in making these assumptions on well-defined structural elements. The second requirement amplifies the effect of the rotational dynamics on the NOE.

6.2.1 Hydrodynamics theory for rotational diffusion rates

The theoretical basis for the influence of molecular rotation on homonuclear NMR relaxation has been reviewed in chapter 5 and should be consulted. This section will explore the current hydrodynamics theories for predicting rotational correlation times, given a hydrodynamic particle of defined shape, and other experimental methods used for determining these correlation times.

The rotational diffusion rate, D_r, for a hydrodynamic particle is given by the rotational analog of the Stokes-Einstein equation for translational diffusion,

$$D_r = \frac{k_b T}{f_r}, \qquad 6.1$$

where k_b is Boltzmann's constant, T is the temperature in Kelvin and f_r is the rotational friction coefficient. It is in the modeling of the rotational friction coefficient that the hydrodynamic shape of the subject is important. For a spheroid,

$$f_r = 8\pi\eta_0 R^3, \qquad 6.2$$

where R is the radius and η_0 is the viscosity of the pure solvent (see the Materials and Methods section of Chapter 4 for a discussion of calculating viscosities for H_2O and D_2O solutions).

For modeling more complex shapes, it is often convenient to express the friction coefficient in terms of a sphere of "equivalent radius", *Re*. This requires the inrtoduction of a new dimensionless frictional coefficient (denoted with a capital F), defined as $F_r = f/f_{sphere,,}$

$$f_r = F_r(8\pi\eta_0 Re^3). \qquad 6.3$$

The *Re* for a cylindrical rod can be calculated using,

$$Re_{(cylinder)} = \left(\frac{2}{2p^2}\right)^{1/3}\left(\frac{L}{2}\right), \qquad 6.4$$

where p is the axial ratio of length to diameter ($p=L/d$). F_r must be defined separately for the two axis of rotation for a cylinder, $F_{r,l}$ and $F_{r,s}$ in which the axis labeled l is the long axis and the axis labeled s is the short axis of a cylinder (Fig. 6.1). Notice that we will define the variables describing the long axis ($D_{r,l}$, and $F_{r,l}$) as that property *about* the long axis. That is, the $D_{r,l}$ of a DNA will be the rotational diffusion rate of the short axis *about* the long axis. It should be noted that in the literature these definitions are sometimes reversed; $D_{r,l}$ may describe the rotational diffusion rate *of* the long axis about the short axis.

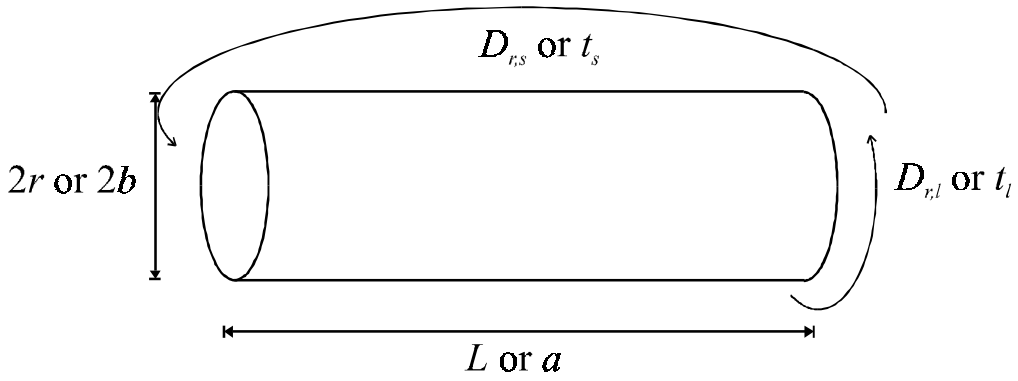

Figure 6.1 Definitions of hydrodynamic variables for a cylinder

$$F_{r,l} = 0.64\left(1 + \frac{0.677}{p} - \frac{0.183}{p^2}\right), \qquad 6.5$$

$$F_{r,s} = \frac{2p^2}{9(\ln p + \delta_a)}, \qquad 6.6$$

with the delta function given by the polynomial approximation as described by Tirado and Garcia de la Torre (1979, 1980),

$$\delta_a = -0.662 + \frac{0.917}{p} - \frac{0.050}{p^2}. \qquad 6.7$$

Equations 6.2, 6.4, 6.5, 6.6 and 6.7 are combined to give functions for $D_{r,s}$ and $D_{r,l}$ in terms of the axial ratio, p, and length,

$$D_{r,l} = \frac{k_b T}{\pi \eta_0 L^3} \cdot \left(\frac{p^2}{0.64 + 0.43328 p^{-1} - 0.11712 p^{-2}}\right), \qquad 6.8$$

$$D_{r,s} = \frac{3k_b T}{\pi \eta_0 L^3} \cdot (\ln p + \delta_a). \qquad 6.9$$

The functions describing the rotational diffusion of a cylinder are shown graphically in figure 6.2 to demonstrates how $D_{r,s}$ and $D_{r,l}$ respond for DNA of size ranging from 5-40 base pairs. Also shown in the graph, are the more NMR-relevant correlation times, t_s and t_l , defined by,

$$t_s = \frac{1}{6D_{r,s}}, \quad t_l = \frac{1}{6D_{r,s}}. \qquad 6.10$$

6.2.2 Experimentally determined correlation times for DNA

Much work has been done on measuring the rotational diffusion rates (D_r) of small and large molecules in solution (Einstein, 1956; Debye, 1929; Perrin, 1934; Perrin, 1936; Alms, *et al*., 1973; Kivelson, 1987; Eimer *et al*., 1990; Eimer & Pecora, 1991). It

has been shown that for some systems these measured rates can be calculated accurately for dilute systems by treating the molecule of interest as a hydrodynamic particle. Many

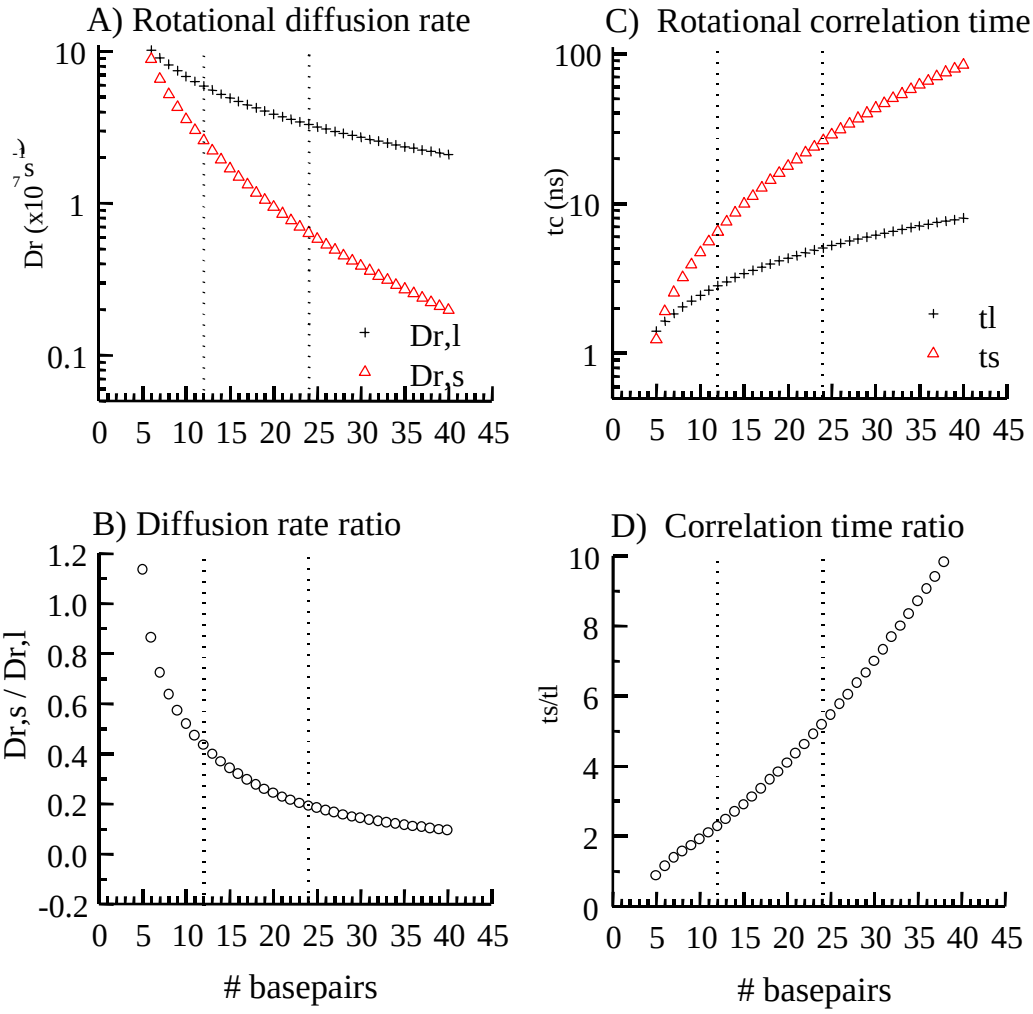

Figure 6.2 Theoretically calculated D_r and t_c values for DNA

Graphs were calculated with equations 6.8 and 6.9 (using the script "hydro.pl", see Chapter 8) at 25° C in 100% D_2O for B-form DNA with hydrodynamic parameters of 3.4 Å rise/bp and a diameter of 20 Å. **A**) Calculated rotational diffusion rates. **B**) Ratios of $D_{r,s}/D_{r,l}$. At 6 base pairs, the length and diameter of DNA is nearly equal, giving a ratio of 1. For larger DNAs, $D_{r,s} < D_{r,l}$. **C**) Correlation times, calculated using $t_c=1/(6*D_r)$. **D**) Correlation time ratios, t_s/t_l, with increasing DNA size. For DNAs larger than 6 base-pairs, $t_s > t_l$.

optical techniques have been developed for measuring the rotational diffusion rates of large molecules (DNAs > 100 bps), such as dichroism and birefringence. However, for accurate measurements of the fast rotational diffusion rates of short oligonucleotides, Pecora *et al.* (1990, 1991) have used a technique known as "Depolarized Dynamic Light Scattering" (DDLS). This technique measures the reorientation relaxation time about the short axis of symmetry ($D_{r,s}$), and is almost completely insensitive to rotation about the long axis ($D_{r,l}$).

Using the DDLS technique, Pecora measured $D_{r,s}$ values of 51.8, 26.1 and 10.3 x 10^6 s^{-1} (t_s values of 3.2, 6.4 and 16.2 ns) for DNAs of sizes 8, 12 and 20 base pairs respectively (Eimer & Pecora, 1991). They showed that these values can be predicted accurately by hydrodynamics theory when modeling DNA as a symmetric top as was presented in section 6.2.1 (Tirado & Garcia de la Torre, 1979, 1980; Tirado, *et al*., 1984; Garcia de la Torre, *et al*., 1984). The hydrodynamic parameters used in their analysis were 3.4 Å rise per base pair and 20 Å diameter. Additionally, it was also found that there was no significant concentration effects for the rotational diffusion measurements for DNA in a concentration range of between 0.1 to ~2.0 mM.

6.2.3 Experimental approach

Analysis of the data presented in this chapter will rely on the technique of back calculating NOE intensities from a structural, rotational and intermolecular dynamic "model" of the molecule in question. A statistical comparison of the simulated NOE intensities and the experimentally measured intensities will evaluate how well the particular model fits the data. The computer program YARM will be used to perform the

calculations (see Chapter 7 for a description of the program) and the YARM scripts used in each calculation can be found in the last section of this chapter.

In order to isolate the effect of the rotational motions on the NOE, the structure and intermolecular dynamics of the samples will be held constant and their rotational motions will be varied. For each rotational motion sampled, the statistical comparison between the simulated and experimental NOEs will be reported. For example, for a truly isotropically rotating molecule, the best fit to the data should occur when the long axis and short axis correlation times are identical; indicating that there is no systematic angular dependence to the cross-relaxation rates between the spins.

6.2.4 Choice of samples

A variety of molecular hydrodynamic shapes were chosen for analysis, ranging from a small sphere to an elongated cylinder. In the world of nucleic acids, these shapes were found in a small 14-nucleotide RNA hairpin (R14) and a 12 and a 24 base pair DNA duplex (D12 and D24). The approximate hydrodynamic shapes of the samples are shown below (Fig. 6.3).

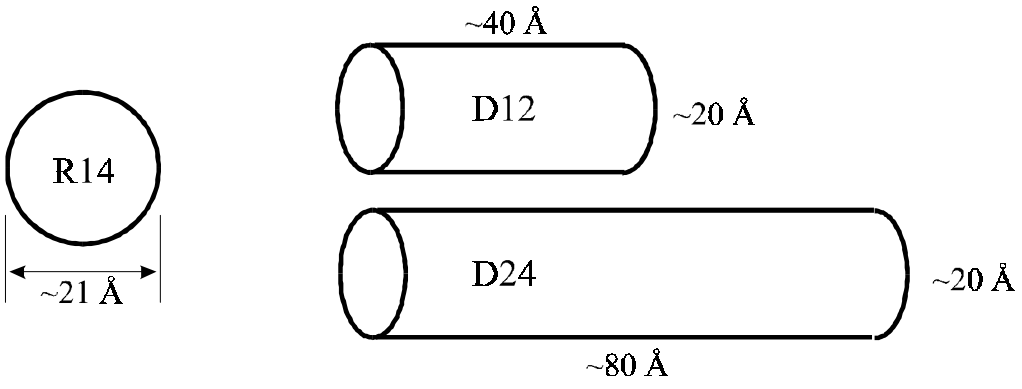

Figure 6.3 Approximate hydrodynamic dimensions of R14, D12 and D24 samples

The R14 RNA is an analog of helix 45 of bacterial 16s rRNA, with a sequence of 5'-GGACCGGAAGGUCC-3'. This RNA has been studied extensively, the hydrodynamical properties of R14 have been examined by measuring the translational diffusion of the RNA (Lapham, et al., 1997) and its solution state structure has also been determined (Rife and Moore, unpublished results).

As was discussed in chapter 4, this RNA can exist in a hairpin conformation in buffers with low salt concentrations and as a dimer in high salt concentration buffers. The hairpin form of the R14 sample was chosen for study because it forms a small compact structure (Rife and Moore, unpublished results), with an approximately spherical hydrodynamic shape, and should closely represent an isotropically rotating molecule. The figure below shows the base pairing for the stem region for R14. The question marks represent, presumably, non standard Watson-Crick A-form RNA structure. Analysis of this RNA involved only the NOEs between protons found in the helix region, specifically G_1, G_2, A_3, C_4, C_5, G_{10}, G_{11}, U_{12}, C_{13} and C_{14} (numbering from 5' to 3'). The NOE data involving the central 4 nucleotides, G_6, G_7, A_8 and A_9 was ignored, due to the possible existence of "interesting" structure or dynamics.

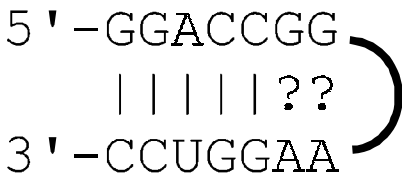

Figure 6.4 14 hairpin

In the analysis of the R14 NOE data a number of assumptions must be made about its molecular model. The helix-stem portion of the molecule will be modeled

structurally as A-form RNA and the intramolecular dynamics will be modeled as rigid. Additionally, the hydrodynamic shape of the RNA will be assumed to be a sphere of radius 10.5 Å.

The two DNAs chosen for study, D12 and D24 were both derived from the sequence found at the EcoR1 restriction site. The first sample, D12, is 5'-CGCGAATTCGCG-3' and is commonly referred to as the "Dickerson dodecamer". There have been a number of structural studies performed of this palindromic DNA, including an X-Ray crystallography (Drew *et al*., 1981) and NMR spectroscopy (Nerdal, *et al*., 1989). Rotational dynamics studies have been reported as well, including results from dynamic light scattering (Eimer, *et al*., 1990; Eimer & Pecora, 1991). Translational diffusion constants have been measured using NMR techniques and discussed in terms of the hydrodynamical modeling of DNA (Lapham, et al., 1997). This DNA is well understood in terms of its structural, rotational and translational dynamics.

The D24 sample is 5'- **CGCGAATTCGCG**CGCGAATTCGCG -3' and, as with the D12 sample, is palindromic. The sequence was constructed by simply duplicating the D12 sequence, with the thought that they would exhibit an identical structure and intramolecular dynamics. The rotational motions, however, should be quite different given that this DNA is twice the length of the D12 DNA.

The symmetry of the DNA molecules is shown below (Fig. 6.5). Notice that the D24 sample contains two "pseudo-symmetric" positions. This causes the protons from the nucleotides near the pseudo-symmetric region to have the same chemical shifts as they do in the D12 sample (Figs. 6.6 and 6.7). We shall assume that, aside from the

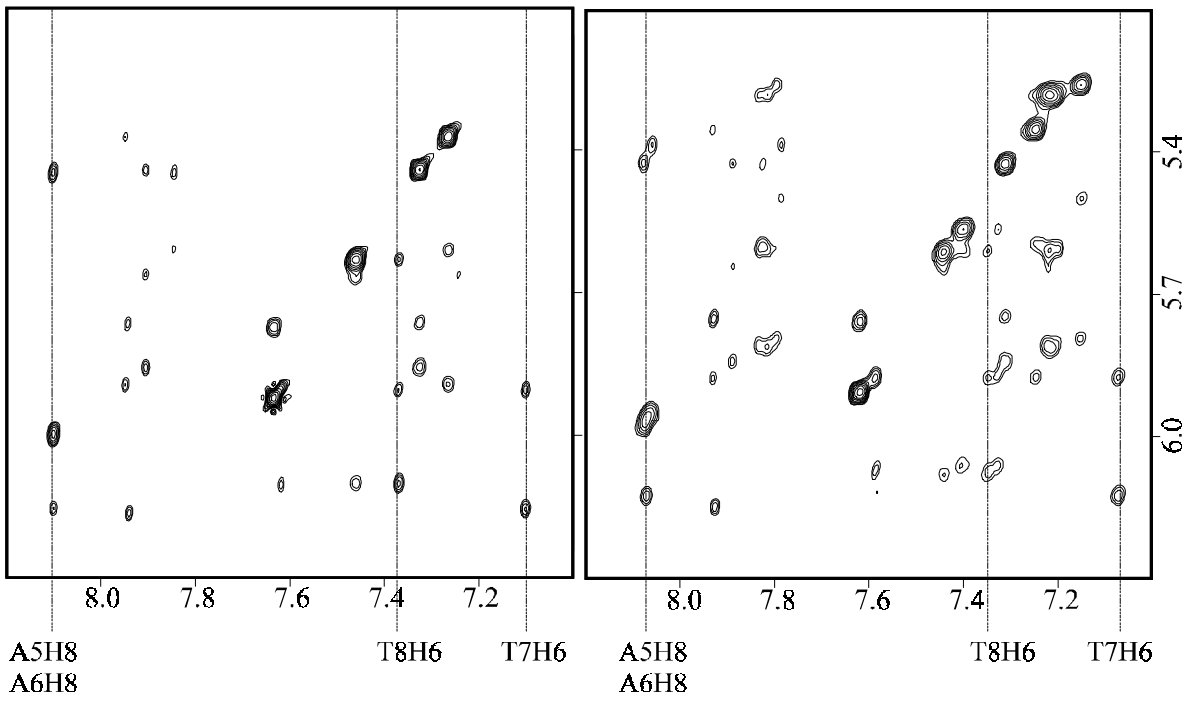

Figure 6.6 D12 and D24 2D NOESY spectra

The 2D NOESY experiments for both the D12 and D24 samples were collected at 25° C using a mixing time of 250 ms and a recycle delay of 30 seconds. Shown is the anomeric-aromatic regions of beth the D12 (left spectra) and D24 (right spectra) samples. The dashed line represent the resonances found in the pseudo-symmetric region of the D24 sample which have identical chemical shifts to the D12 sample.

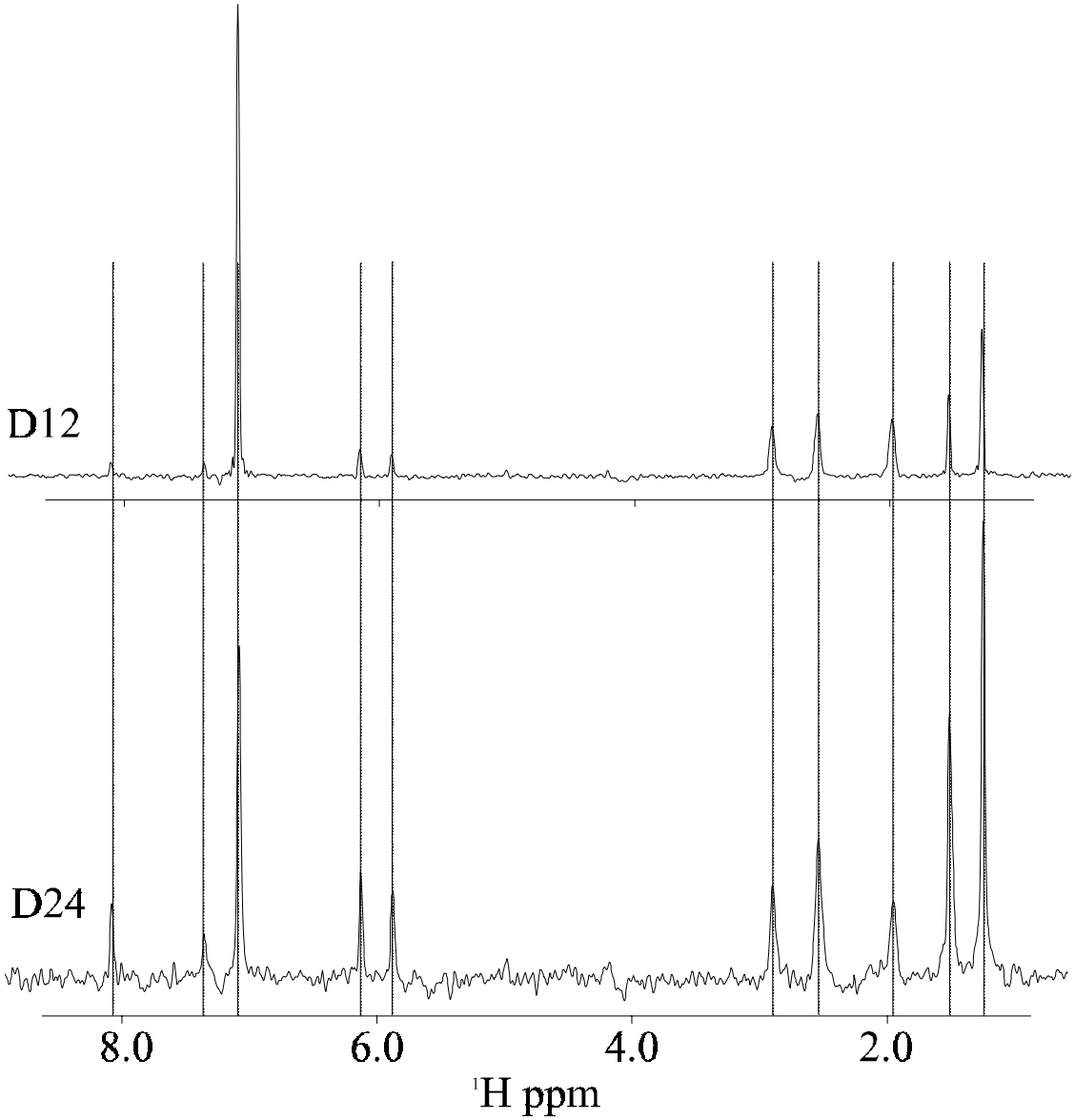

Figure 6.7 T7 H6 1D slice of 2D NOESY

A 1D slice through the thymidine 7 H6 proton from the 2D NOESY spectra for the D12 and D24 samles. The chemical shifts of the crosspeaks are identical between the two samples.

central few G:C base pairs on the D24 sample, the structural and dynamical properties of the D12 and D24 samples are similar.

D12: 5'-GCGCAA TTGCGC-3'
3'-CGCGTT AACGCG-5'

D24: 5'-GCGCAA TTGCGC GCGCAA TTGCGC-3'
3'-CGCGTT AACGCG CGCGTT AACGCG-5'

Figure 6.5 Symmetry in the D12 and D24 samples

The assumed hydrodynamic parameters for the two DNAs are 3.4Å rise per base pair and 20Å diameter, as was confirmed from the translational diffusion rate experiments presented in Chapter 4. This gives a length of 40.8Å and 81.6Å for the D12 and D24 samples respectively as shown below.

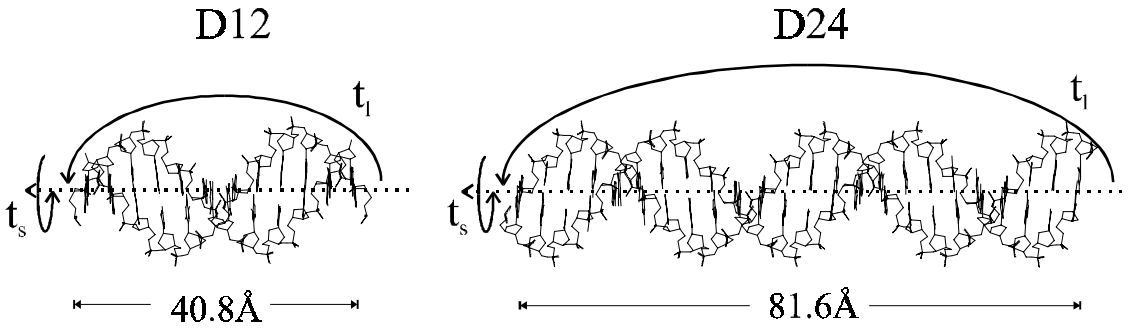

Figure 6.8 Hydrodynamic parameters for the D12 and D24 samples

It should be noted that Jason Rife provided the data for the R14 samples. Any discrepancies in the interpretation of the data, however, lie solely with the author of this thesis.

6.3 Results

This chapter evaluates the effect of different rotational motions on the NOE. This is accomplished by back calculating the simulated NOE intensities and comparing them to experimentally measured values. In order to simulate the NOEs, the computer program YARM will be utilized. Use of the program is described in greater detail in chapter 7, but the theoretical consideration of the calculations are presented in chapter 5. The anisotropic definition of the spectral density function (Woessner, 1962) will be used in these simulations.

6.3.1 Cross-relaxation rate simulations for anisotropic rotation

For an isotropically rotating molecule, all spin pair vectors experience the same rotational diffusion rate and a single "correlation time", t_c, will accurately describe this motion. The rotational motions of the molecule give rise to dipolar relaxation effects between the dipole pair, which can be measured experimentally as a NOE crosspeak in a NOESY experiment. Thus, for a molecule undergoing isotropic rotation, there will be no coordinated "angular dependence" to the cross-relaxation rates between each dipole pair.

However, for a molecule undergoing anisotropic rotation, the rotational diffusion rate each dipole pair vector experiences will depend on the angle the vector makes with respect to the principal axis of rotation (denoted the β_{ij} angle). There will now be a coordinated "angular dependence" to any dipolar relaxation coupling between spin pairs. In terms of the cross-relaxation rates, this effect can be modeled (Fig. 6.9). By changing the long axis correlation time (t_l) with respect to the short axis correlation time (t_s), the cross-relaxation rate (σ_{ij}) is shown to have a strong angular dependence with respect to

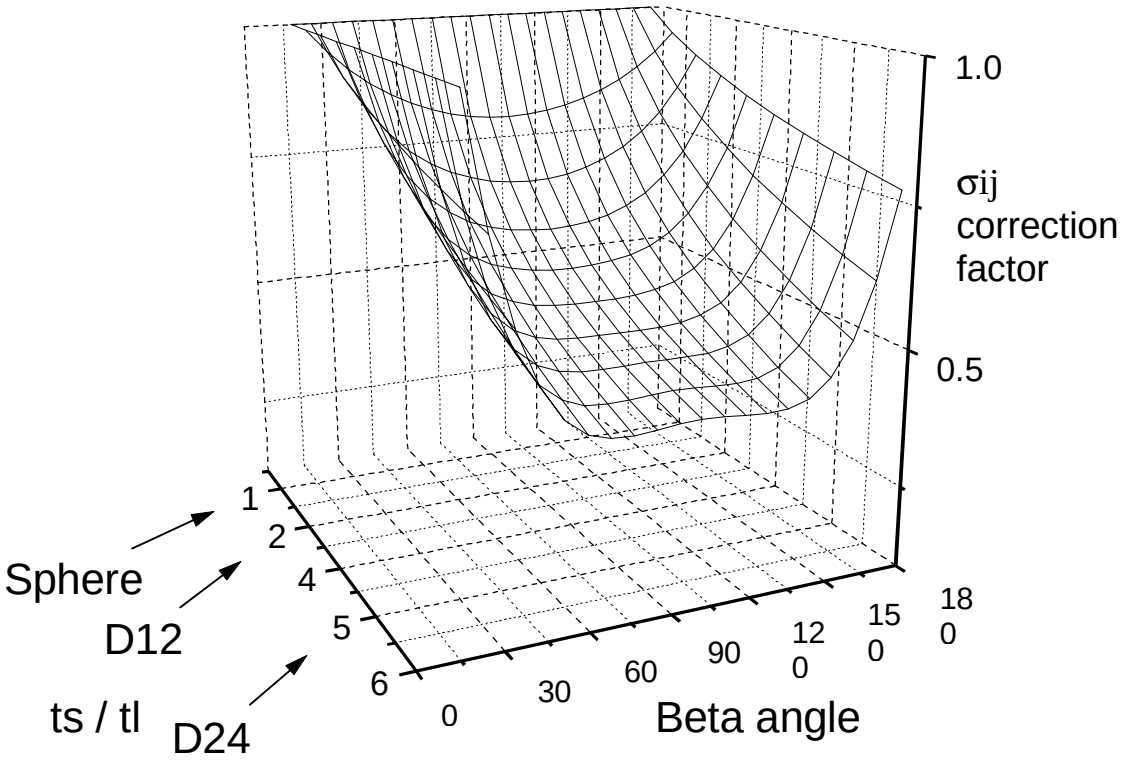

Figure 6.9 Cross-relaxation rate correction factor

As the ratio of the short to long axis correlation time increases, an angular dependence with respect to the principal rotation axis for the cross-relaxation rate is predicted. For the sphere, ts/tl = 1 and there is no angular dependence to sij. For a 12 mer DNA (~40Å x ~20Å) ts/tl ≈ 6.5/2.8 ≈ 2 and for a 24 mer DNA ts/tl ≈ 5. An atom pair vector parallel (0 degrees) to the principal axis of rotation for a 24 mer DNA experiences approximately twice the cross-relaxation rate as a atom pair vector perpendicular (90 degrees) to the principal axis. These values are reported as relative to isotropic rotation with the ts correlation time.

the principal axis of rotation. For a molecule with a $t_s \approx 5t_l$ (such as a 24 base pair DNA), the ratio of the cross-relaxation rates of a spin pair parallel : perpendicular to the principal axis is approximately 2. Since the cross-relaxation rates give rise to the NOE, this effect should be experimentally measurable.

6.3.2 R14 sample

The R14 experimental data was obtained from a 2D NOESY experiment collected at 30° C using a mixing time of 300 ms and a recycle delay of 9 s. A total of 23 well-resolved NOESY crosspeaks (see section 6.5.3 for the volumes list) between protons found in the helix stem region (see Fig. 6.4) of the RNA were used in the analysis. The structure of the helix stem is assumed to be A-form (section 6.5.4).

The rotational hydrodynamics theory (using the program "hydro.pl", see Chap. 8) can be used to predict the rotational diffusion rate, and thus the correlation time, of the R14 sample. Assuming the RNA is a sphere of diameter 21 Å, equation 6.2 predicts a $D_r = 1.48 \times 10^8\ s^{-1}$, which gives a $t_c = 1.1$ ns (for temp = 30° C, in D_2O).

The results of the analysis of the experimentally measured versus the simulated NOEs are shown in figure 6.10 assuming an isotropic rotation model. As the correlation time is varied from 0.1 to 10 ns, the fit of the simulated to the experimental NOEs is plotted. The best fit occurs for a $t_c \approx 0.7$ ns, which is in good agreement (within the experimental and modeling errors) with the predicted value.

To determine if there was any systematic, coordinated angular dependence to the cross-relaxation rates between the spin pairs in the R14 sample, an anisotropic rotation "surface plot" was calculated (Fig. 6.11). In this analysis, the long and short axis correlation times are varied from 0.1 to 10 ns (the X and Y axis respectively) and the

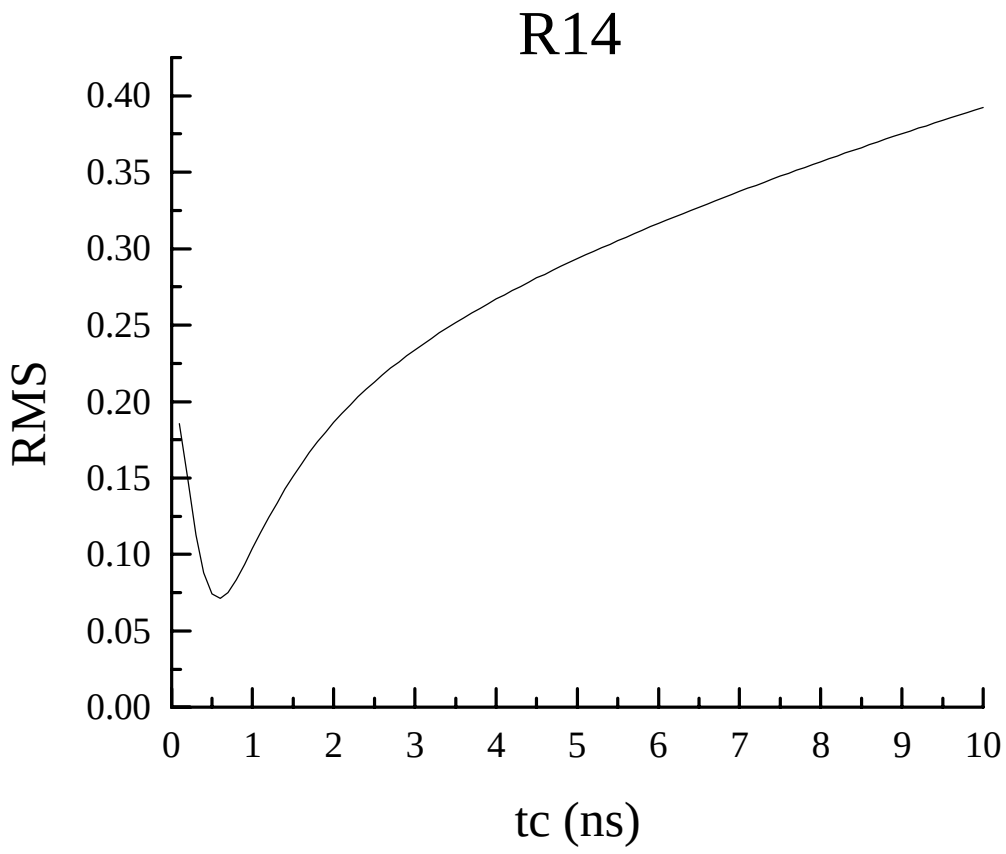

Figure 6.10 R14 isotropic correlation time plot

Graph of the RMS between the experimental NOE data for R14 and the back-calculated NOE data, assuming an A-form RNA with rigid intramolecular dynamics. Using the isotropic definition of the spectral density function, the correlation time of the molecule is varied from 0.1 to 10 ns.

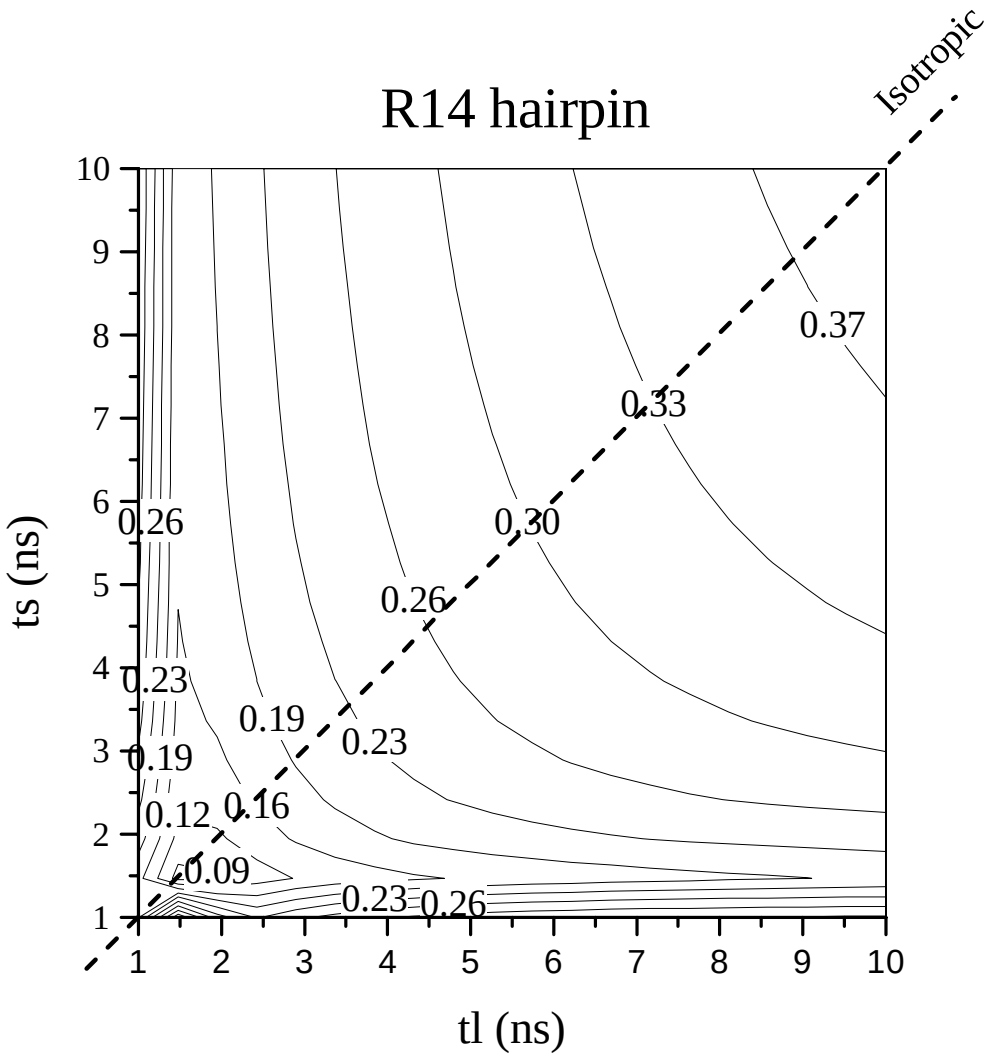

Figure 6.11 R14 anisotropic correlation time "surface plot"

The X and Y axis represent the long and short axis correlation times used in the anisotropic rotation definition of the spectral density function. The Z-axis of the surface plot is the RMS between the experimental and simulated NOESY crosspeak volumes, a minimum in the RMS represents a good fit between the simulated and experimental data. The dashed line represents the position in the graph where $t_s=t_l$, the rotation is isotropic. The simulations were run for a standard A-from RNA at 30° C with a mixing time of 300 ms.

RMS between the experimental and simulated NOEs is graphed on the Z-axis. A "trough" in the surface plot represents a minimum RMS, and a best fit rotational model. Clearly the minimum lies close to the "isotropic line" (where $t_l = t_s$) and modeling the rotational motions as anisotropic gives a worse fit to the data. There is no angular dependence to the measured NOEs for R14, and it is well represented as an isotropically rotating molecule.

6.3.3 D12 sample

A total of 117 well-resolved (234 symmetric) NOESY crosspeaks were used in the analysis of the D12 sample (see section 6.5.3). The structure of the D12 was assumed to be the NMR derived structure (see section 6.5.5) and rigid.

The rotational motions of the D12 sample are predicted using equations 6.5 and 6.6 and assuming the DNA is a cylindrical hydrodynamic particle with dimensions 20 Å by 40.8 Å. This predicts that the D12 DNA has a $D_{r,l} \approx 5.92\text{x}10^7\ \text{s}^{-1}$ $D_{r,s} \approx 2.58\text{x}10^7\ \text{s}^{-1}$ and a $t_l \approx 2.82$ ns, $t_s \approx 6.46$ ns.

The anisotropic rotation surface plot for the simulated versus experimental data for D12 is shown in figure 6.12. Unlike the R14 sample, the minimum RMS is not found on the isotropic line, rather it is off the diagonal in a region where the $t_s > t_l$. The graph shows that the RMS is not very sensitive to the t_s correlation time, but is very sensitive to the t_l correlation time. The predicted rotational dynamics for the D12 fall in the region of the minimum RMS, indicating that both the theoretical and experimental data indicate that the D12 sample is experiencing anisotropic rotation.

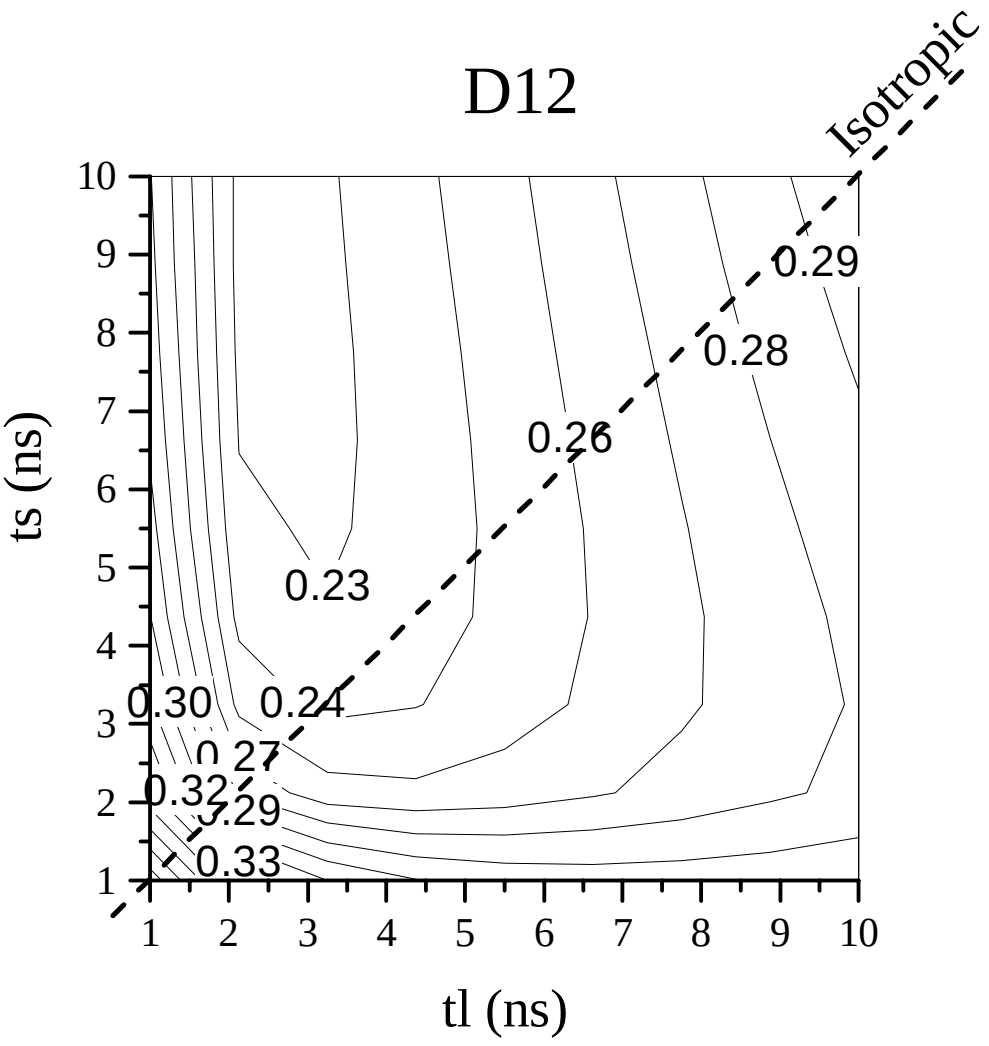

Figure 6.12 D12 anisotropic correlation time "surface plot"

The X and Y axis represent the long and short axis correlation times used in the anisotropic rotation definition of the spectral density function. The Z-axis of the surface plot is the RMS between the experimental and simulated NOESY crosspeak volumes, a minimum in the RMS represents a good fit between the simulated and experimental data. The dashed line represents the position in the graph where $t_s=t_l$, the rotation is isotropic. The simulations were run at 25° C with a mixing time of 250 ms.

Hydrodynamics theory predicts a correlation time of 2.8 ns about the long axis and 6.5 about the short axis for D12.

6.3.4 D24 sample

A total of 21 well-resolved (42 symmetric) crosspeaks were used in the analysis of the D24 sample (see section 6.5.3), from the pseudo-symmetric region of the DNA (the A-T base pairs). We reasoned that since the crosspeaks from this region of the DNA have exactly the same chemical shifts as for the D12 sample (see Figs. 6.6 and 6.7), the structure and intramolecular dynamics in this region was probably similar.

The predicted rotational correlation times for the D24 samples are $D_{r,l} \approx 3.30\text{x}10^7$ s^{-1} $D_{r,s} \approx 0.64\text{x}10^7$ s^{-1} and a $t_l \approx 5.05$ ns, $t_s \approx 26.2$ ns (temp = 25° C, D_2O). The hydrodynamics theory suggests that the long axis rotates about 5 times for every short axis rotation.

The anisotropic rotation surface plot for D24 is shown in figure 6.13 (note that the range of the t_l and t_s values was increased to 40 ns as compared to the R14 and D12 surface plots). A tough of minimum RMS is seen where $t_s > t_l$, as would be expected. The minimum is not, however, exactly where the predicted values would suggest. Clearly the D24 sample is undergoing an anisotropic rotation, but the correlation time about the long axis appears to be much bigger than predicted.

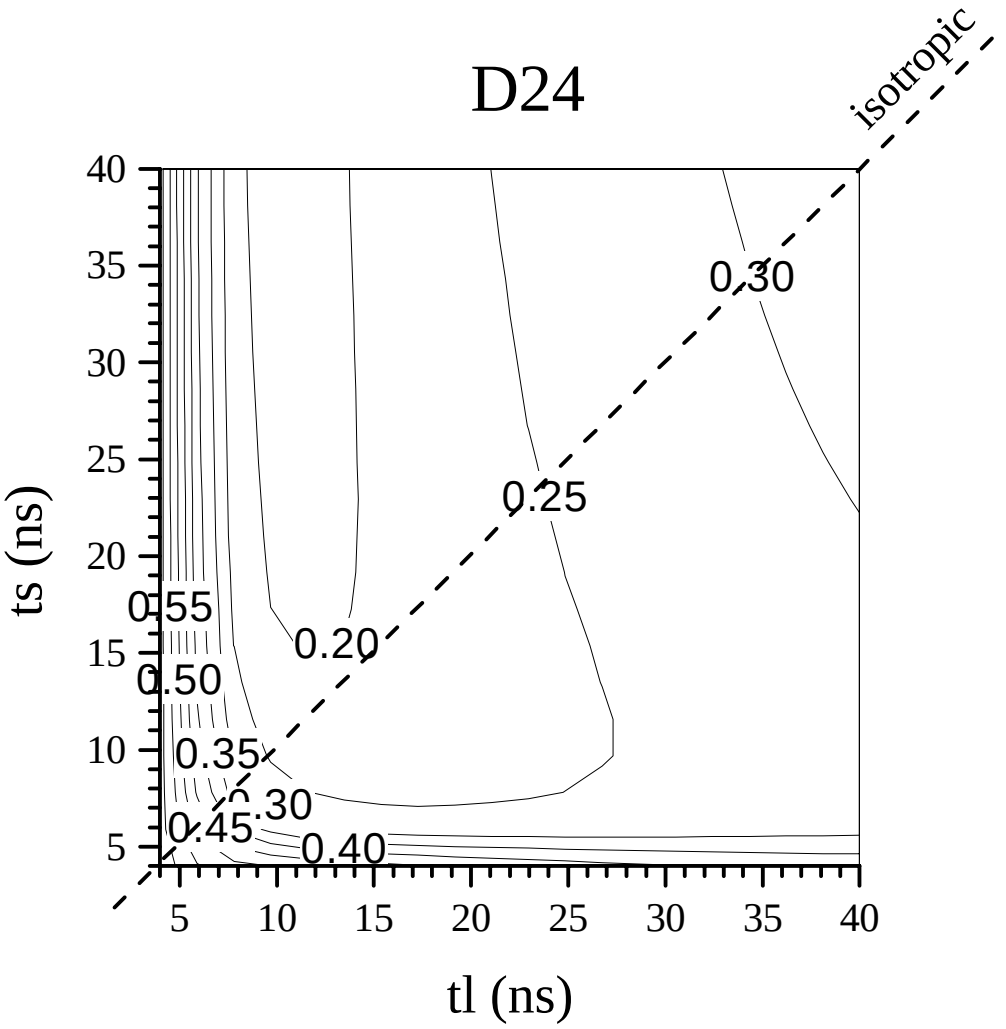

Figure 6.13 D24 anisotropic correlation time surface plot

The X and Y axis represent the long and short axis correlation times used in the anisotropic rotation definition of the spectral density function. The Z-axis of the surface plot is the RMS between the experimental and simulated NOESY crosspeak volumes, a minimum in the RMS represents a good fit between the simulated and experimental data. The dashed line represents the position in the graph where t_s=t_l, the rotation is isotropic. The simulations were run 25° C with a mixing time of 250 ms.

Hydrodynamics theory predicts a t_l=5ns and t_s=26ns. The minimum RMS appears at approximately a long axis correlation time of 10 - 12 ns, and a wide range of short axis correlation times.

6.4 Discussion

The pattern and intensities of NOE crosspeaks in the 2D NOESY experiment represent a wealth of information on the relaxation processes that occur in a molecule. The rates of these dipolar relaxation processes are dependent on three molecular components: the structure of the molecule (r_{ij}), the intramolecular dynamics of the molecule (dr_{ij}/dt) and the rotational motions of the molecule (t_c). These structural and motional components are represented in the relaxation matrix, **R**, as the spectral density function, *J*. Thus, in order to model accurately the relaxation matrix, an accurate definition of the spectral density function is required.

In this chapter, we attempt to deconvolute the effect of molecular rotational dynamics on the relaxation matrix, and ultimately on the NOE intensities. In order to accomplish this, we have quantitated the NOE crosspeak volumes from three NMR samples, which should exhibit different rotational motions. These experimentally measured NOEs are then compared to theoretically simulated NOEs, to ascertain whether the rotational properties of the molecules can be seen in the experimental NMR data itself.

The small RNA hairpin, R14, is predicted to rotate in an isotropic manner. The analysis of the NOEs arising from the helix stem region of the RNA confirms this. The NOE intensities between the measured spin pairs fit well with simulated NOE data using the isotropic definition of the spectral density function. When the anisotropic rotation spectral density function is examined, the back-calculated NOE intensities are a worse fit to the measured experimental data.

The DNA samples, D12 and D24, are predicted to have rotational motions described by two correlation times, one about the long axis and one about the short axis. The data indicate that the predictions are correct, the simulated NOE data is a better fit to the experimental when using the anisotropic rotation spectral density function using a $t_s > t_l$.

The D12 sample shows remarkable agreement between the predicted $t_l \approx 2.8$ ns and $t_s \approx 6.5$ ns and the minimum in the anisotropic rotation surface plot (Fig. 6.12). It can be said that these correlation times probably represent the rotational motions of this DNA well.

The predicted correlation times for the D24 sample, however, do not seem to align with the minimum in the surface plot (Fig. 6.13). The predicted $t_l \approx 5$ ns, while the minimum in the data appears at $t_l \approx$ 10-12 ns. One explanation of this discrepancy is that the sample may undergo normal mode bending along the length of the DNA (Zimm, 1956). This bending may cause the long axis rotational diffusion rate to be slower, due to the increased frictional coefficient about the long axis from the bent DNA shape, as shown below in figure 6.14. As the length of the DNA increases, the angular fluctuations due to the normal mode bending in DNA increases. Thus, the D24 DNA would suffer from this more than the D12 sample.

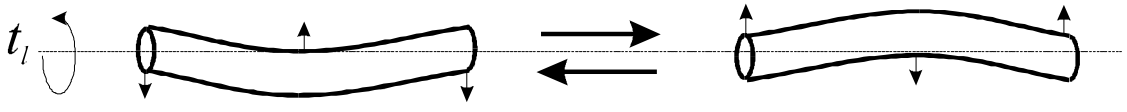

Figure 6.14 Normal mode bending motions of DNA

In conclusion, we are able to observe the effect of molecular tumbling in the experimentally measured NOE data. This is an important consideration for biomolecular NMR spectroscopists as they investigate larger extended shape nucleic acid molecules, as the intensities of their NOESY crosspeaks will have an additional "angular dependence" to them.

6.5 Materials and Methods

6.5.1 Sample preparation

The R14 RNA, sequence 5'- GGACCGGAAGGUCC-3' contained 3 methylated nucleotides in the hairpin loop at positions 6,8 and 9: m^2G6, $m_6{}^2$A8 and $m_2{}^6$A9. The R14 RNA was prepared by chemical synthesis using methylated phosphoramidites (Rife, J.P., Cheng, C.S., Moore, P.B., Strobel, S.A., submitted manuscript). The methylations should have no appreciable affect on the NOE data for the stem region of the RNA since they are only found in the hairpin loop. The R14 was 2.2 mM in 50 mM NaCl, 5 mM cacodylate (pH 6.3), 1mM EDTA buffer.

The two DNA samples were prepared on an Applied Biosystems 380B DNA synthesizer and purified using denaturing PAGE techniques. Concentrations were determined by UV absorbance measurements at 260nm wavelength and calculated using a dinucleotide stacking extinction coefficient formula. The DNA sequences were (5' to 3') D12:CGCGAATTCGCG and D24:CGCGAATTCGCGCGCGAATTCGCG. Both D12 and D24 were palindromic to alleviate any problems with stoichiometry. The samples were dialyzed against 20mM sodium phosphate (pH 7.0) and 100mM NaCl for two days, exchanging the dialysis buffer every 12 hours. Both samples were placed in a Shigemi (Shigemi Corp., Tokyo Japan) NMR tube in a 170 µl volume, which equated to about a 1 cm sample height. The samples were then lyophylized and resuspended in 100.0 atom % D_2O from Aldrich (cat #26,978-6) to the same final sample volume of 170 µl.

6.5.2 NMR experimental

The 2D NOESY data collected for the RNA and DNA samples was performed using a modified version of the canned noesy.c pulse sequence that is supplied with the Varian spectrometers. The modification involved removing the homospoil pulse in the mixing time and replacing it with a z-axis gradient pulse. This insures better removal of COSY-type single and double quantum coupling.

Data for both the D12 and D24 samples were collected at 25º C with a recycle delay of 30 s to insure complete z-magnetization relaxation between scans. Data for the R14 sample was collected at 30º C with w recycle delay of 9.2 s. For all samples, 1024 complex points were collected in the direct dimension, and at least 300 complex points was collected in the indirect dimension. Data processing was accomplished in the direct dimension by applying a 1024 point, 90 degree shifted sine-bell curve to all FIDS. Processing in the indirect dimension was accomplished by applying a 300 point, 90 degree shifted sine-bell curve to all FIDS.

Two-dimensional NOESY experiments were collected for each sample at mixing times ranging from 50-400 ms using very long recycle delays (10–30s) to insure complete Z axis magnetization recovery between scans. Sample spectra are shown in figure 6.6 and a sample one-dimensional slice through the H6 resonance of Thymine #7 for each sample is shown in figure 6.7. Chemical shift assignments for the D12 sample come from those previously published (Nerdal, *et al*., 1989) and D24 assignments followed by simply overlaying the spectra.

6.5.3 Volumes lists

The next few pages contain the volumes experimentally measured for each of the three samples along with the simulated volumes using the best rotational correlation time model.

R14 experimental and simulated NOE volume data

Simulations used: tc = 0.7 ns

```
YARM v0.9 February 22, 1998
Found 30 atoms
Principal axis vector components Ax=0.00 Ay=0.00 Az=1.00
Stats: found 30 in the first dimension of the reference hash
Stats: Finished
Pairwise statistical analysis:
           RMS = 0.0751
      R-factor = 0.1240
      Q-factor = 0.0620
Q^(1/6)-factor = 0.0373

Atom_I          atom_j          rij   exp   sim
A 1 GUA H8      A 1 GUA H1'     3.73  0.32  0.34
A 1 GUA H1'     A 2 GUA H8      4.32  0.38  0.31
A 2 GUA H8      A 2 GUA H1'     3.73  0.33  0.25
A 2 GUA H1'     A 3 ADE H8      4.32  0.30  0.32
A 3 ADE H2      A 4 CYT H1'     3.83  0.48  0.28
A 3 ADE H1'     A 3 ADE H8      3.70  0.28  0.25
A 3 ADE H1'     A 4 CYT H6      4.30  0.18  0.32
A 4 CYT H5      A 4 CYT H6      2.46  2.36  2.36
A 4 CYT H6      A 4 CYT H1'     3.52  0.39  0.29
A 5 CYT H6      A 5 CYT H1'     3.52  0.31  0.29
A 5 CYT H1'     A 6 GUA H8      4.32  0.09  0.31
A 6 GUA H1'     A 6 GUA H8      3.73  0.30  0.25
A 7 GUA H1'     A 7 GUA H8      0.00  2.60  0.00
A 9 ADE H1'     A 9 ADE H8      0.00  0.40  0.00
A 10 GUA H1'    A 10 GUA H8     3.73  0.21  0.25
A 10 GUA H1'    A 11 GUA H8     4.32  0.27  0.31
A 11 GUA H1'    A 11 GUA H8     3.73  0.29  0.25
A 11 GUA H1'    A 12 URI H6     4.28  0.20  0.33
A 12 URI H5     A 12 URI H6     2.42  2.31  2.52
A 13 CYT H5     A 13 CYT H6     2.46  2.33  2.36
A 13 CYT H1'    A 14 CYT H6     4.30  0.29  0.33
A 14 CYT H5     A 14 CYT H6     2.46  2.63  2.37
A 14 CYT H6     A 14 CYT H1'    3.52  0.36  0.29
```

D12 experimental and simulated NOE volume data

Simulations used: ts = 2.8 ns tl = 6 ns

```
YARM v0.9 February 22, 1998
F95_Merge_Vols_Peaks: WARNING, negative volume, skipping
F95_Merge_Vols_Peaks: WARNING, negative volume, skipping
Found 110 atoms
Simulating NOE volumes using anisotropic-rigid...
Principal axis vector components Ax=-0.00 Ay=-0.35 Az=0.94
Stats: found 110 in the first dimension of the reference hash
Stats: Finished
Pairwise statistical analysis:
           RMS = 0.2138
      R-factor = 0.3036
      Q-factor = 0.1518
Q^(1/6)-factor = 0.0689
```

Atom_I	atom_j	rij	exp	sim
A 1 CYT H6	A 1 CYT H2''	4.27	2.70	1.89
A 1 CYT H6	A 1 CYT H1'	3.66	3.50	1.88
A 1 CYT H6	A 1 CYT H2'	2.95	9.81	3.00
A 1 CYT H1'	A 1 CYT H2''	2.37	10.85	10.36
A 1 CYT H1'	A 1 CYT H2'	3.04	3.04	7.87
A 1 CYT H2'	A 1 CYT H2''	1.80	22.37	26.30
A 1 CYT H2'	A 2 GUA H8	3.45	1.34	1.66
A 2 GUA H1'	A 2 GUA H8	3.86	0.19	3.37
A 2 GUA H1'	A 2 GUA H2''	3.05	8.71	7.35
A 2 GUA H1'	A 2 GUA H2'	2.38	5.73	11.54
A 2 GUA H1'	A 3 CYT H5	4.12	1.68	1.46
A 2 GUA H1'	A 3 CYT H6	2.95	1.45	3.82
A 2 GUA H2'	A 3 CYT H5	3.35	2.14	2.48
A 2 GUA H2'	A 3 CYT H6	2.85	0.97	3.97
A 2 GUA H8	A 3 CYT H5	4.26	0.65	0.90
A 2 GUA H2''	A 3 CYT H5	4.09	2.82	1.51
A 2 GUA H2''	A 3 CYT H6	4.35	2.50	2.21
A 3 CYT H2''	A 3 CYT H6	3.83	5.12	5.43
A 3 CYT H2''	A 3 CYT H1'	2.40	14.22	8.25
A 3 CYT H2''	A 3 CYT H2'	1.79	24.57	21.20
A 3 CYT H2''	A 4 GUA H8	2.91	1.91	4.20
A 3 CYT H1'	A 3 CYT H6	3.72	1.50	1.64
A 3 CYT H1'	A 3 CYT H2'	3.07	5.26	5.75
A 3 CYT H1'	A 4 GUA H8	4.23	0.41	1.10
A 3 CYT H2'	A 3 CYT H5	4.39	2.83	1.87
A 3 CYT H2'	A 3 CYT H6	2.35	12.78	9.11
A 3 CYT H2'	A 4 GUA H8	3.15	1.43	3.59
A 3 CYT H5	A 3 CYT H6	2.46	14.77	14.63
A 4 GUA H1'	A 4 GUA H8	3.98	0.68	1.89
A 4 GUA H1'	A 4 GUA H2''	3.06	13.61	7.59
A 4 GUA H1'	A 4 GUA H2'	2.37	11.52	11.32
A 4 GUA H1'	A 5 ADE H8	3.61	2.17	2.07
A 4 GUA H8	A 4 GUA H2''	2.45	4.96	10.09
A 4 GUA H8	A 4 GUA H2'	3.84	7.93	5.75
A 4 GUA H8	A 5 ADE H8	4.74	0.60	0.64
A 5 ADE H2'	A 5 ADE H2''	1.77	20.50	26.00
A 5 ADE H2'	A 5 ADE H1'	2.37	5.95	10.17
A 5 ADE H2	A 6 ADE H2	3.76	2.54	1.74
A 5 ADE H2	B 9 CYT H1'	4.18	0.39	0.63
A 5 ADE H2''	A 5 ADE H1'	3.05	13.44	7.66
A 6 ADE H8	A 6 ADE H1'	3.90	1.17	1.27
A 6 ADE H8	A 6 ADE H2'	4.12	8.49	2.43
A 6 ADE H8	A 7 THY H6	4.78	0.88	1.15
A 6 ADE H8	A 7 THY H7	3.60	7.00	5.36
A 6 ADE H2'	A 6 ADE H2''	1.76	19.95	14.86
A 6 ADE H2'	A 6 ADE H1'	2.38	7.82	9.18
A 6 ADE H2'	A 7 THY H7	4.13	6.61	4.42
A 6 ADE H1'	A 6 ADE H2''	3.04	10.19	6.52
A 6 ADE H1'	A 7 THY H6	3.84	1.93	2.47
A 6 ADE H1'	A 7 THY H7	5.24	0.40	1.42
A 6 ADE H2''	A 7 THY H6	3.08	7.16	5.54
A 6 ADE H2''	A 7 THY H7	3.39	5.84	5.92
A 6 ADE H2	B 8 THY H1'	3.95	0.89	0.87
A 7 THY H1'	A 7 THY H6	3.74	1.26	2.20
A 7 THY H1'	A 7 THY H2''	2.38	12.84	7.83
A 7 THY H1'	A 7 THY H2'	3.05	9.26	5.58
A 7 THY H1'	A 8 THY H6	3.56	1.17	2.42
A 7 THY H2''	A 7 THY H2'	1.78	20.28	17.97
A 7 THY H2''	A 8 THY H7	3.90	6.61	6.10
A 7 THY H6	A 7 THY H7	2.93	13.83	13.54
A 7 THY H6	A 7 THY H2'	2.11	8.76	11.14
A 7 THY H6	A 8 THY H6	4.42	1.08	2.26
A 7 THY H6	A 8 THY H7	3.44	6.56	6.03
A 7 THY H7	A 8 THY H7	3.96	4.01	9.88
A 7 THY H2'	A 8 THY H6	3.27	4.62	6.18
A 7 THY H2'	A 8 THY H7	3.35	6.12	6.64
A 8 THY H6	A 8 THY H7	2.94	12.51	13.84
A 8 THY H6	A 8 THY H1'	3.72	2.38	2.27

```
A 8 THY H6     A 8 THY H2'     2.15 13.06 11.64
A 8 THY H6     A 9 CYT H5      3.56  1.36  1.90
A 8 THY H6     A 9 CYT H6      4.64  2.18  1.55
A 8 THY H7     A 9 CYT H5      4.16  0.51  2.73
A 8 THY H1'    A 8 THY H2''    2.38 11.79  8.42
A 8 THY H1'    A 8 THY H2'     3.05  7.38  5.97
A 8 THY H1'    A 9 CYT H6      3.75  1.78  1.98
A 8 THY H1'    B 6 ADE H2      3.94  0.89  0.89
A 8 THY H2'    A 8 THY H2''    1.78 23.20 20.17
A 8 THY H2'    A 9 CYT H6      3.45  4.15  5.03
A 8 THY H2'    A 9 CYT H5      3.44  3.39  2.51
A 8 THY H2''   A 9 CYT H6      2.39  5.01  7.86
A 8 THY H2''   A 9 CYT H5      3.62  3.36  3.01
A 9 CYT H5     A 9 CYT H6      2.43 14.71 13.13
A 9 CYT H5     A 9 CYT H2''    5.70  3.92  1.12
A 9 CYT H5     A 9 CYT H2''    4.39  2.63  2.33
A 9 CYT H6     A 9 CYT H2''    3.74  5.73  6.82
A 9 CYT H6     A 9 CYT H1'     3.72  2.67  2.13
A 9 CYT H6     A 9 CYT H2''    2.25 13.33 10.96
A 9 CYT H1'    A 9 CYT H2''    2.37 10.74  8.86
A 9 CYT H1'    A 9 CYT H2'     3.05  4.39  6.18
A 9 CYT H1'    A 10 GUA H8     3.60  0.73  2.19
A 9 CYT H1'    B 5 ADE H2      4.16  0.39  0.66
A 9 CYT H2'    A 10 GUA H8     3.23  2.03  5.21
A 9 CYT H2''   A 10 GUA H8     2.50  2.28  7.82
A 10 GUA H2'   A 10 GUA H8     3.68 11.19  8.13
A 10 GUA H2'   A 10 GUA H1'    2.37  7.88  9.69
A 10 GUA H2'   A 11 CYT H6     2.76  1.82  4.37
A 10 GUA H2''  A 10 GUA H8     2.24  6.06 13.06
A 10 GUA H2''  A 10 GUA H1'    3.05  8.26  6.75
A 10 GUA H2''  A 11 CYT H6     4.14  3.03  2.57
A 10 GUA H8    A 10 GUA H1'    3.91  1.07  2.18
A 10 GUA H8    A 11 CYT H5     4.62  0.71  0.44
A 10 GUA H8    A 11 CYT H6     5.14  0.32  0.69
A 10 GUA H1'   A 11 CYT H5     4.86  0.67  0.63
A 10 GUA H1'   A 11 CYT H6     3.37  2.35  2.14
A 11 CYT H1'   A 11 CYT H6''   3.70  1.61  2.10
A 11 CYT H1'   A 11 CYT H2''   2.40 14.77  9.49
A 11 CYT H1'   A 11 CYT H2'    3.06  4.91  6.90
A 11 CYT H1'   A 12 GUA H8     4.39  0.69  1.39
A 11 CYT H2'   A 11 CYT H5     4.41  1.66  1.66
A 11 CYT H2'   A 11 CYT H6     2.45 13.88  8.36
A 11 CYT H2'   A 11 CYT H2''   1.79 22.26 25.47
A 11 CYT H2''  A 12 GUA H8     3.54  1.94  4.58
A 11 CYT H2''  A 11 CYT H6     3.91  5.04  5.31
```

```
A 11 CYT H5    A 11 CYT H6     2.46 13.44 15.06
A 11 CYT H6    A 12 GUA H8     5.55  0.13  0.66
A 12 GUA H1'   A 12 GUA H8     3.93  0.92  1.38
A 12 GUA H1'   A 12 GUA H2''   3.00  5.38  9.39
A 12 GUA H1''  A 12 GUA H2'    2.32 15.92 13.46
A 12 GUA H2'   B 1 CYT H6      1.79 30.03 31.07
B 1 CYT H2'    B 1 CYT H2''    2.95  9.81  3.00
B 1 CYT H2'    B 1 CYT H1'     1.79 22.37 26.32
B 1 CYT H2''   B 1 CYT H1'     3.04  3.04  7.86
B 1 CYT H2''   B 2 GUA H8      3.45  1.34  1.66
B 1 CYT H2''   B 1 CYT H6      4.26  2.70  1.90
B 1 CYT H2''   B 1 CYT H1'     2.37 10.85 10.33
B 1 CYT H6     B 1 CYT H1'     3.66  3.50  1.88
B 1 CYT H1'    B 2 GUA H8      3.86  0.19  3.37
B 2 GUA H1'    B 2 GUA H2''    3.05  8.71  7.35
B 2 GUA H1'    B 2 GUA H2'     2.38  5.73 11.55
B 2 GUA H1'    B 3 CYT H5      4.12  1.68  1.46
B 2 GUA H1'    B 3 CYT H6      2.95  1.45  3.83
B 2 GUA H2''   B 3 CYT H5      4.09  2.82  1.51
B 2 GUA H2''   B 3 CYT H6      4.35  2.50  2.20
B 2 GUA H8     B 3 CYT H5      4.26  0.65  0.90
B 2 GUA H2'    B 3 CYT H5      3.35  2.14  2.48
B 2 GUA H2'    B 3 CYT H6      2.85  0.97  3.97
B 3 CYT H5     B 3 CYT H6      2.46 14.77 14.63
B 3 CYT H5     B 3 CYT H2'     4.39  2.83  1.87
B 3 CYT H6     B 3 CYT H2''    3.83  5.12  5.43
B 3 CYT H6     B 3 CYT H1'     3.72  1.50  1.64
B 3 CYT H6     B 3 CYT H2'     2.35 12.78  9.11
B 3 CYT H2'    B 3 CYT H2''    1.79 24.57 21.22
B 3 CYT H2'    B 3 CYT H1'     3.07  5.26  5.76
B 3 CYT H2'    B 4 GUA H8      3.15  1.43  3.58
B 3 CYT H1'    B 3 CYT H2''    2.40 14.22  8.26
B 3 CYT H1''   B 4 GUA H8      4.23  0.41  1.10
B 3 CYT H2''   B 4 GUA H8      2.91  1.91  4.19
B 3 CYT H2''   B 4 GUA H8      2.46  4.96 10.09
B 4 GUA H2''   B 4 GUA H1'     3.06 13.61  7.61
B 4 GUA H8     B 4 GUA H1'     3.98  0.68  1.89
B 4 GUA H8     B 4 GUA H2'     3.84  7.93  5.74
B 4 GUA H8     B 5 ADE H8      4.74  0.60  0.64
B 4 GUA H1'    B 4 GUA H2'     2.36 11.52 11.37
B 4 GUA H1'    B 5 ADE H8      3.61  2.17  2.07
B 5 ADE H1'    B 5 ADE H2''    3.05 13.44  7.67
B 5 ADE H1'    B 5 ADE H2'     2.37  5.95 10.18
B 5 ADE H2''   B 5 ADE H2'     1.77 20.50 26.00
B 5 ADE H2     B 6 ADE H2      3.77  2.54  1.70
```

```
B 9 CYT H2''    B 9 CYT H1'     2.36 10.74  8.94
B 9 CYT H2''    B 10 GUA H8     2.49  2.28  7.92
B 9 CYT H5      B 9 CYT H6      2.44 14.71 12.80
B 9 CYT H6      B 9 CYT H1'     3.73  2.67  2.10
B 9 CYT H1'     B 10 GUA H8     3.59  0.73  2.25
B 10 GUA H2'    B 10 GUA H8     3.70 11.19  7.79
B 10 GUA H2'    B 10 GUA H1'    2.37  7.88  9.68
B 10 GUA H2'    B 11 CYT H6     2.76  1.82  4.37
B 10 GUA H8     B 10 GUA H2''   2.27  6.06 12.29
B 10 GUA H8     B 10 GUA H1'    3.91  1.07  2.11
B 10 GUA H8     B 11 CYT H5     4.63  0.71  0.44
B 10 GUA H8     B 11 CYT H6     5.14  0.32  0.67
B 10 GUA H8''   B 10 GUA H1'    3.04  8.26  6.88
B 10 GUA H2''   B 11 CYT H6     4.13  3.03  2.64
B 10 GUA H1'    B 11 CYT H5     4.86  0.67  0.63
B 10 GUA H1'    B 11 CYT H6     3.37  2.35  2.14
B 11 CYT H2'    B 11 CYT H5     4.43  1.66  1.63
B 11 CYT H2'    B 11 CYT H6     2.47 13.88  8.05
B 11 CYT H2''   B 11 CYT H2''   1.78 22.26 25.28
B 11 CYT H2'    B 11 CYT H1'    3.05  4.91  7.20
B 11 CYT H2'    B 12 GUA H8     3.53  1.94  4.64
B 11 CYT H5     B 11 CYT H6     2.45 13.44 15.38
B 11 CYT H6     B 11 CYT H1'    3.71  1.61  2.09
B 11 CYT H6     B 11 CYT H2''   3.92  5.04  5.14
B 11 CYT H6     B 12 GUA H8     5.54  0.13  0.65
B 11 CYT H2''   B 11 CYT H1'    2.38 14.77  9.93
B 11 CYT H1'    B 12 GUA H8     4.35  0.69  1.46
B 12 GUA H8     B 12 GUA H2''   1.78 30.03 30.60
B 12 GUA H2''   B 12 GUA H1'    2.32 15.92 13.55
B 12 GUA H1'    B 12 GUA H2''   2.99  5.38  9.48
B 12 GUA H2''   B 12 GUA H1'    3.91  0.92  1.41
B 12 GUA H1'
```

```
B 6 ADE H1'     B 6 ADE H8      3.90  1.17  1.27
B 6 ADE H1'     B 6 ADE H2''    3.04 10.19  6.53
B 6 ADE H1'     B 6 ADE H2'     2.38  7.82  9.17
B 6 ADE H1'     B 7 THY H6      3.84  1.93  2.47
B 6 ADE H1'     B 7 THY H7      5.24  0.40  1.42
B 6 ADE H8      B 6 ADE H2'     4.12  8.49  2.42
B 6 ADE H8      B 7 THY H6      4.78  0.88  1.14
B 6 ADE H8      B 7 THY H7      3.60  7.00  5.34
B 6 ADE H2'     B 6 ADE H2''    1.76 19.95 14.87
B 6 ADE H2'     B 7 THY H7      4.13  6.61  4.42
B 6 ADE H2''    B 7 THY H6      3.08  7.16  5.56
B 6 ADE H2''    B 7 THY H7      3.39  5.84  5.92
B 7 THY H6      B 7 THY H7      2.93 13.83 13.56
B 7 THY H6      B 7 THY H1'     3.74  1.26  2.19
B 7 THY H6      B 7 THY H2'     2.11  8.76 11.10
B 7 THY H6      B 8 THY H6      4.42  1.08  2.27
B 7 THY H6      B 8 THY H7      3.44  6.56  6.04
B 7 THY H7      B 8 THY H7      3.96  4.01  9.83
B 7 THY H1'     B 7 THY H2''    2.38 12.84  7.81
B 7 THY H1'     B 7 THY H2'     3.05  9.26  5.58
B 7 THY H1'     B 8 THY H6      3.56  1.17  2.43
B 7 THY H2'     B 7 THY H2''    1.77 20.28 17.99
B 7 THY H2'     B 8 THY H6      3.27  4.62  6.22
B 7 THY H2'     B 8 THY H7      3.35  6.12  6.67
B 7 THY H2''    B 8 THY H7      3.90  6.61  6.13
B 8 THY H1'     B 8 THY H2'     3.05  7.38  5.94
B 8 THY H1'     B 8 THY H6      3.72  2.38  2.25
B 8 THY H1'     B 8 THY H2''    2.38 11.79  8.33
B 8 THY H1'     B 9 CYT H6      3.73  1.78  2.08
B 8 THY H2'     B 8 THY H6      2.15 13.06 11.50
B 8 THY H2'     B 8 THY H2''    1.78 23.20 20.02
B 8 THY H2'     B 9 CYT H5      3.45  3.39  2.53
B 8 THY H2''    B 9 CYT H6      3.43  4.15  5.38
B 8 THY H2''    B 9 CYT H5      3.62  3.36  3.07
B 8 THY H2''    B 9 CYT H6      2.35  5.01  8.41
B 8 THY H6      B 8 THY H7      2.94 12.51 13.88
B 8 THY H6      B 9 CYT H5      3.56  1.36  1.91
B 8 THY H6      B 9 CYT H6      4.63  2.18  1.62
B 8 THY H7      B 9 CYT H5      4.16  0.51  2.74
B 9 CYT H2'     B 9 CYT H5      4.41  2.63  2.20
B 9 CYT H2'     B 9 CYT H6      2.26 13.33 10.51
B 9 CYT H2'     B 9 CYT H1'     3.04  4.39  6.32
B 9 CYT H2'     B 10 GUA H8     3.23  2.03  5.34
B 9 CYT H2''    B 9 CYT H5      5.69  3.92  1.09
B 9 CYT H2''    B 9 CYT H6      3.74  5.73  6.67
```

D24 experimental and simulated NOE volume data

Simulations used: ts = 12 ns tl = 26 ns

```
YARM v0.9 February 22, 1998
Found 40 atoms
Simulating NOE volumes using anisotropic-rigid...
Principal axis vector components Ax=-0.00 Ay=-0.35 Az=0.94
Stats: found 40 in the first dimension of the reference hash
Stats: Finished
Pairwise statistical analysis:
           RMS = 0.2398
      R-factor = 0.2812
      Q-factor = 0.1406
Q^(1/6)-factor = 0.0544
```

Atom_i	atom_j	rij	exp	sim
A 5 ADE H2'	A 5 ADE H2''	1.77	13.32	11.98
A 5 ADE H2	A 8 ADE H2	0.00	9.89	0.00
A 6 ADE H8	A 6 ADE H1'	3.90	2.90	3.40
A 6 ADE H8	A 7 THY H6	4.78	2.90	4.26
A 6 ADE H2'	A 6 ADE H2''	1.76	10.44	6.80
A 6 ADE H1'	A 7 THY H6	3.84	3.88	5.13
A 6 ADE H2''	A 7 THY H6	3.08	5.42	6.18
A 7 THY H1'	A 7 THY H6	3.74	2.61	4.63
A 7 THY H2''	A 7 THY H2'	1.78	12.65	7.74
A 7 THY H2''	A 8 THY H7	3.90	21.55	15.04
A 7 THY H6	A 7 THY H7	2.93	21.99	20.68
A 7 THY H6	A 7 THY H2'	2.11	4.70	7.66
A 7 THY H6	A 8 THY H6	4.42	2.53	6.07
A 7 THY H6	A 8 THY H7	3.44	14.92	16.17
A 7 THY H7	A 8 ADE H8	0.00	17.63	0.00
A 7 THY H7	A 8 ADE H2''	0.00	18.23	0.00
A 7 THY H7	A 8 ADE H2'	0.00	19.95	0.00
A 7 THY H7	A 8 THY H7	3.96	19.45	32.86
A 7 THY H2'	A 8 THY H7	3.35	15.64	15.56
A 8 THY H6	A 8 THY H7	2.94	21.66	20.31
A 8 THY H2'	A 8 THY H2''	1.78	15.58	7.66
B 5 ADE H2'	B 5 ADE H2''	1.77	13.32	11.98
B 5 ADE H2	B 8 ADE H2	0.00	9.89	0.00
B 6 ADE H2'	B 6 ADE H2''	1.76	10.44	6.81
B 6 ADE H2''	B 7 THY H6	3.08	5.42	6.18
B 6 ADE H8	B 6 ADE H1'	3.90	2.90	3.40
B 6 ADE H8	B 7 THY H6	4.78	2.90	4.26
B 6 ADE H1'	B 7 THY H6	3.84	3.88	5.14
B 7 THY H6	B 7 THY H7	2.93	21.99	20.69
B 7 THY H6	B 7 THY H1'	3.74	2.61	4.62
B 7 THY H6	B 7 THY H2'	2.11	4.70	7.66
B 7 THY H6	B 8 THY H6	4.42	2.53	6.09
B 7 THY H6	B 8 THY H7	3.44	14.92	16.17
B 7 THY H7	B 8 ADE H8	0.00	17.63	0.00
B 7 THY H7	B 8 ADE H2''	0.00	18.23	0.00
B 7 THY H7	B 8 ADE H2'	0.00	19.95	0.00
B 7 THY H7	B 8 THY H7	3.96	19.45	32.74
B 7 THY H2'	B 7 THY H2''	1.77	12.65	7.76
B 7 THY H2'	B 8 THY H7	3.35	15.64	15.59
B 7 THY H2''	B 8 THY H7	3.90	21.55	15.08
B 8 THY H2''	B 8 THY H2'	1.78	15.58	7.61
B 8 THY H6	B 8 THY H7	2.94	21.66	20.36

6.5.4 R14 structure

```
filename: rife.pdb
segments:1  residues:14
segid  num res  alpha    beta    gamma     eps      zeta     chi      nu0      nu1      nu2      nu3      nu4      P       numax   pucker
-----  --- ---  ------  -------  -------  -------  -------  -------  -------  -------  -------  -------  -------  ------  ------  --------
    A   1 GUA    0.00 -179.87   47.43 -151.72  -73.59 -158.02   3.38  -25.82   37.26  -36.18   20.72   13.58   38.34  C3'-endo
    A   2 GUA  -62.10 -179.87   47.44 -151.67  -73.64 -158.01   3.43  -25.85   37.27  -36.15   20.67   13.50   38.33  C3'-endo
    A   3 ADE  -62.09 -179.88   47.44 -151.68  -73.64 -158.97   3.42  -25.84   37.28  -36.18   20.70   13.53   38.34  C3'-endo
    A   4 CYT  -62.07 -179.88   47.41 -151.73  -73.61 -166.06   3.38  -25.84   37.30  -36.20   20.74   13.58   38.38  C3'-endo
    A   5 CYT  -62.07 -179.87   47.43 -151.74  -73.59 -166.06   3.43  -25.87   37.31  -36.20   20.71   13.52   38.37  C3'-endo
    A   6 GUA  -62.12 -179.87   47.44    0.00    0.00 -158.00   3.43  -25.85   37.27  -36.16   20.68   13.51   38.33  C3'-endo
    A   9 CYT  129.63 -179.87   47.43 -151.68  -73.69 -166.06   3.35  -25.80   37.27  -36.21   20.77   13.63   38.35  C3'-endo
    A  10 GUA  -62.06 -179.87   47.44 -151.64  -73.64 -158.03   3.41  -25.83   37.26  -36.16   20.69   13.54   38.33  C3'-endo
    A  11 GUA  -62.07 -179.87   47.44 -151.72  -73.60 -158.01   3.41  -25.85   37.29  -36.20   20.72   13.55   38.36  C3'-endo
    A  12 URI  -62.10 -179.88   47.44 -151.72  -73.64 -165.74   3.35  -25.78   37.25  -36.19   20.76   13.64   38.33  C3'-endo
    A  13 CYT  -62.07 -179.87   47.43 -151.68  -73.66 -166.06   3.35  -25.77   37.24  -36.17   20.74   13.63   38.32  C3'-endo
    A  14 CYT  -62.08 -179.87   47.43    0.00    0.00 -166.06   3.38  -25.82   37.26  -36.18   20.72   13.58   38.34  C3'-endo
```

6.5.5 D12 and D24 structure

```
filename: dick_nmr.pdb
segments:2  residues:12
segid  num res  alpha    beta    gamma     eps      zeta      chi      nu0      nu1      nu2      nu3      nu4      P      numax   pucker
------ --- --- -------- -------- -------- -------- -------- -------- -------- -------- -------- -------- -------- ------- ------- --------
     A   1 CYT    0.00   -50.84  115.20  -178.52   -86.71  -144.71   -34.63    22.02    -3.03   -16.79    31.89   95.06   34.36  O4'-endo
     A   2 GUA  -62.52  -164.95   56.19   143.08   -93.18   -85.89   -26.97    35.05   -30.43    15.89     6.55  150.65   34.91  C2'-endo
     A   3 CYT  -78.42  -158.07   80.15   176.32   -73.87  -125.61   -28.29    31.64   -24.24     8.79    11.93  139.79   31.74  C1'-exo
     A   4 GUA  -64.41  -153.01   26.73   167.33   -98.36   -92.97   -30.34    35.67   -28.23    11.91    11.10  143.12   35.29  C1'-exo
     A   5 ADE  -73.32  -169.50   61.78   176.47  -107.50  -101.72   -33.46    34.92   -23.94     5.58    17.10  132.68   35.31  C1'-exo
     A   6 ADE  -99.73   167.22  101.00  -167.86   -99.75  -116.22   -31.69    34.06   -24.25     6.81    15.26  135.17   34.19  C1'-exo
     A   7 THY  -21.54  -176.60    2.04  -178.70   -98.46  -109.75   -26.57    33.74   -28.64    14.51     7.38  148.89   33.45  C2'-endo
     A   8 THY  -54.47   172.28   45.60   176.07   -94.16  -114.33   -35.83    35.33   -22.32     2.71    20.23  127.76   36.44  C1'-exo
     A   9 CYT  -70.52  -173.80   54.48   169.58   -82.79  -117.65   -32.84    31.13   -18.89     0.88    19.49  125.14   32.81  C1'-exo
     A  10 GUA  -80.01  -148.25   38.02   162.60   -96.57   -92.14   -28.28    34.91   -29.08    13.79     8.68  147.03   34.67  C2'-endo
     A  11 CYT  -58.95  -173.02   62.42  -170.26  -106.55  -129.53   -34.45    30.93   -16.87    -2.19    22.57  119.95   33.80  C1'-exo
     A  12 GUA  -57.51   162.98   68.25     0.00     0.00  -125.51   -30.59    14.68     4.85   -22.84    33.04   81.61   33.21  O4'-endo

     B   1 CYT    0.00   -60.27  115.24  -178.52   -86.75  -144.65   -34.59    22.00    -3.01   -16.80    31.86   95.04   34.33  O4'-endo
     B   2 GUA  -62.45  -164.96   56.11   143.12   -93.12   -85.86   -26.91    34.99   -30.40    15.89     6.52  150.69   34.86  C2'-endo
     B   3 CYT  -78.46  -158.07   80.17   176.30   -73.86  -125.56   -28.25    31.60   -24.23     8.82    11.88  139.86   31.70  C1'-exo
     B   4 GUA  -64.37  -153.02   26.70   167.34   -98.37   -92.93   -30.33    35.62   -28.20    11.89    11.13  143.10   35.27  C1'-exo
     B   5 ADE  -73.36  -169.50   61.81   176.50  -107.56  -101.74   -33.47    34.89   -23.90     5.51    17.15  132.60   35.31  C1'-exo
     B   6 ADE  -99.78   167.21  101.01  -167.85   -99.75  -116.19   -31.64    33.99   -24.20     6.80    15.25  135.16   34.13  C1'-exo
     B   7 THY  -21.49  -176.61    1.98  -178.70   -98.46  -109.76   -26.51    33.69   -28.60    14.52     7.32  148.95   33.38  C2'-endo
     B   8 THY  -54.44   172.27   45.66   176.09   -94.09  -114.37   -35.91    35.32   -22.22     2.60    20.31  127.55   36.45  C1'-exo
     B   9 CYT  -70.59  -173.77   54.46   169.63   -82.73  -117.63   -32.58    31.04   -18.98     1.08    19.19  125.55   32.64  C1'-exo
     B  10 GUA  -79.94  -148.26   38.09   162.69   -96.73   -92.15   -28.13    34.83   -29.05    13.85     8.57  147.18   34.57  C2'-endo
     B  11 CYT  -58.79  -173.05   62.15  -170.07  -106.43  -129.22   -34.05    30.66   -16.85    -2.03    22.12  120.27   33.42  C1'-exo
     B  12 GUA  -57.54   162.98   68.23     0.00     0.00  -125.42   -30.46    14.68     4.81   -22.76    32.88   81.64   33.09  O4'-endo
```

6.5.6 YARM scripts

The next two pages contain the YARM scripts used to calculate the correlation plots presented in this chapter, one for calculating the isotropic correlation plot (Fig. 6.10) and the other for calculating the anisotropic correlation time plots (Figs. 6.11-6.13). The third YARM script was used to generate the statistical analysis for a specific rotational model and was used to make the volume lists found in section 6.5.3.

Anisotropic rotation correlation time plot

```
#!/usr/local/bin/perl
# yarm Yet Another Relaxation Matrix program

# Read in the library file:
require "/usr/local/yarm/yarm_lib.pl";

##############################################
# Set variables
##############################################
$pdb_file = "d12_b.pdb";
$f95_vol_file = "d12_30s.vols";
$f95_peak_file = "d12_30s.peaks";

$sfreq = 600;
$vol0 = 100;
$tmix = 0.2;

$debug = 0;

##############################################
# Run yarm modules
##############################################
print "$yarm_version\n";
# Read in PDB file, calculate rij matrix and principal axis

# Get non-exchangeable nucleic acid protons from a PDB file
%xyz = &Pdb_Read_All( $pdb_file );
%xyz = &Get_Atom_Type( \%xyz, \%nonX_NA );
%xyz = &Pseudo_Methyl(\%xyz);

%rij = &Rij_Hash( \%xyz, 0, 10 );

($Ax, $Ay, $Az ) = Principal_Axis( \%xyz );
printf ("The inertia tensor principal axis is Ax=%4.3f
Ay=%4.3f  Az=%4.3f\n",
        $Ax, $Ay, $Az);

# Read in experimental volumes
%vol_exp = &F95_Read_Merge( $f95_vol_file, $f95_peak_file );
%vol_exp = &Make_Symm_Molecule( A, B, \%vol_exp );
```

```
open (REPORT, "> tl_ts_aniso.out" );

for ($ts = 0.1; $ts < 10; $ts += 0.25) {
for ($tl = 0.1; $tl < 10; $tl += 0.25) {

        print "Working on tl=$tl and ts=$ts\n";

        # Calculate anisotropic rotation volumes
        %vol_sim = &Sim_Vol( $sfreq, $tmix, $vol0, \%xyz,
\%rij, $tl, $ts,
                $Ax, $Ay, $Az, \%S );

        # Normalize the experimental volumes by comparing h5-h6
volumes
        %vol_exp = &Norm_Hash( \%vol_exp, \%vol_sim);

        # Determine gobs of information out about the pairwise
volume
        # comparison between the experimental and isotropic
volumes
        ( $rms, $r, $q, $q6 ) = &Stats( \%vol_exp, \%vol_sim );

        print "finished tl=$tl ts=$ts RMS=$rms\n\n";
        print REPORT "$rms\n";
}
}

close REPORT;
```

Isotropic rotation correlation time plot

```
#!/usr/local/bin/perl
# yarm Yet Another Relaxation Matrix program

# Read in the library file:
require "/usr/local/yarm/yarm_lib.pl";

##############################################
# Set variables
##############################################
$pdb_file = "dick_b.pdb";
$f95_vol_file = "d12_30s.vols";
$f95_peak_file = "d12_30s.peaks";

$sfreq = 600;
$vol0 = 100;
$tmix = 0.2;

debug = 0;

##############################################
# Run yarm modules
##############################################
print "$yarm_version\n";
# Read in PDB file, calculate rij matrix and principal axis

# Get non-exchangeable nucleic acid protons from a PDB file
%xyz = &Pdb_Read_All( $pdb_file );
%xyz = &Get_Atom_Type( \%xyz, \%nonX_NA );
%xyz = &Pseudo_Methyl(\%xyz);

%rij = &Rij_Hash( \%xyz, 0, 10 );

# Read in experimental volumes
%vol_exp = &F95_Read_Merge( $f95_vol_file, $f95_peak_file );
%vol_exp = &Make_Symm_Molecule( A, B, \%vol_exp );

open (REPORT, "> tc_iso.out" );
for ($tc = 0.1; $tc < 10; $tc += 0.1) {

    print "Working on tc=$tc\n";
```

```
    # Calculate isotropic rotation volumes
%vol_sim = &Sim_Vol( $sfreq, $tmix, $vol0, \%xyz, \%rij, $tl
);

    # Normalize the experimental volumes by comparing h5-h6
volumes
    %vol_exp = &Norm_Hash( \%vol_exp, \%vol_sim );

    # Determine gobs of information out about the pairwise
volume
    # comparison between the experimental and isotropic volumes
    ( $rms, $r_factor, $q, $q6 ) = &Stats( \%vol_exp,
\%vol_sim);

    print "finished tc=$tc  RMS=$rms\n\n";
    print REPORT "$tc $rms\n";
}

close REPORT;
```

YARM script to generate a volumes listing

```
#!/usr/local/bin/perl
require "/usr/local/yarm/yarm_lib.pl";

################################################
# Define variables
################################################
$pdb_file = shift;
$sfreq = 600;
$vol0 = 100;
$tmix = 0.25;

$tl = 2.8;
$ts = 6.5;
$S = 1;

$f95_vol_file = "d12_30s.vols";
$f95_peak_file = "d12_30s.peaks";

# $f95_vol_file = "d24_200_selected_vols.txt";
# $f95_peak_file = "d24_200_selected_peaks.txt";

# Set to 0 for no debugging messages
# Set to 1 for a few debugging messages
# set to 2 for TONS of debugging messages (lots!)
$debug = 0;

################################################
# Call YARM subroutines
################################################
print "$yarm_version\n";

# Get non-exchangeable nucleic acid protons from a PDB file
%xyz = &Pdb_Read_All( $pdb_file );
%xyz = &Get_Atom_Type( \%xyz, \%nonX_NA );
%xyz = &Pseudo_Methyl(\%xyz);

foreach $atom ( keys %xyz ) { $S{$atom} = $S; }

# Measure distances of all atom pairs between
# 0 to 10 angstroms
%rij  = &Rij_Hash( \%xyz );


# Read in experimental volumes
%vol_exp = &F95_Read_Merge( $f95_vol_file, $f95_peak_file );
# Convert the experimental volumes to include segids A and B
# We have to do this b/c this DNA is a symmetric molecule
%vol_exp = &Make_Symm_Molecule( A, B, \%vol_exp );

@atoms = keys %vol_exp;
print "Found ",$#atoms+1," atoms\n";

# ANISOTROPIC ROTATION
# Calculate the principal axis of rotation vector
print "Simulating NOE volumes using anisotropic-rigid...\n";
( $Ax, $Ay, $Az ) = Principal_Axis( \%xyz );
printf ("Principal axis vector components Ax=%4.2f Ay=%4.2f
Az=%4.2f\n", $Ax, $Ay, $Az);
%vol_sim = &Sim_Vol( $sfreq, $tmix, $vol0, \%xyz, \%vol_exp,
    $tl, $ts, $Ax, $Ay, $Az, \%S );

# ISOTROPIC ROTATION
# print "Simulating NOE volumes using isotropic-rigid...\n";
# %vol_sim = &Sim_Vol( $sfreq, $tmix, $vol0, \%xyz, \%rij, $tc
);

# Normalize the experimental volumes to the simulated volumes
%vol_exp = &Norm_Hash( \%vol_exp, \%vol_sim );

# Calculate statistics between the experimental and simulated
volume sets
$debug=1;
( $rms, $r, $q, $q6 ) = &Stats( \%vol_exp, \%vol_sim );

################################################
# Print a nice report
################################################
# Print the final "report" rms value
print   "Pairwise statistical analysis:\n";
printf ("           RMS = %5.4f\n", $rms);
printf ("      R-factor = %5.4f\n", $r);
printf ("      Q-factor = %5.4f\n", $q);
printf ("Q^(1/6)-factor = %5.4f\n", $q6);
print "\n";

@atoms_i = keys %vol_exp;
@atoms_i = Sortme ( \@atoms_i );
```

```
foreach $atom_i ( @atoms_i ) {
    @atoms_j = keys %{ $vol_exp{$atom_i} };
    @atoms_j = Sortme ( \@atoms_j );
    foreach $atom_j ( @atoms_j ) {
        next if ( ($used{$atom_i}{$atom_j}) or
             ($used{$atom_j}{$atom_i}) );
        $used{$atom_i}{$atom_j} = "t";

        $v_e = $vol_exp{$atom_i}{$atom_j};
        $v_s = $vol_sim{$atom_i}{$atom_j};
        $rij = $rij{$atom_i}{$atom_j};
        printf ("%-15s %-15s %4.2f %5.2f %5.2f\n",
            $atom_i, $atom_j, $rij, $v_e, $v_s);

    }
}
exit;
```

6.6 References

Alms GR, Bauer DR, Brauman JI, Pecora R. 1973. *J. Chem. Phys 59*:5310-5321.

Debye P. 1929. *Polar Molecules*. New York: Dover.

Drew HR, Wing RM, Takano T, Broka C, Tanaka S, Itakura K, Dickerson RE. 1981. Structure of a B-DNA dodecamer: conformation and dynamics. *PNAS 78*:2179-2182.

Eimer W, Pecora R. 1991. Rotational and translational diffusion of short rodlike molecules in solution: Oligonucleotides. *J. Chem. Phys. 94*:2324-2329.

Eimer W, Williamson JR, Boxer SG, Pecora R. 1990. Characterization of the overall and internal dynamics of short oligonucleotides by depolarized dynamic light scattering and NMR relaxation measurements. *Biochemistry 29*:799-811.

Einstein A. 1956. *Investigations into the Theory of the Brownian Movement*. New York: Dover.

Kivelson D. 1987. *Rotational Dynamics of Small and Macromolecules.* Heidelberg: Springer.

Lapham J, Rife J, Moore PB, Crothers DM. 1997. Measurement of diffusion constants for nucleic acids by NMR. *J. Biomolecular NMR 10*:255-262.

Nerdal W, Hare DR, Reid BR. 1989. Solution structure of the *Eco*RI DNA sequence: refinement of NMR-derived distance geometry structures by NOESY spectrum back-calculations. *Biochemistry 28*:10008-10021.

Perrin F. 1934. *J. Phys. Rad. 5*:497.

Perrin F. 1936. *J. Phys. Rad. 7*:1.

Tirado MM, Martinez CL, Garcia de la Torre J. 1984. Comparison of theories for the translational and rotational diffusion coefficients of rod-like macromolecules. Application to short DNA fragments. *J Chem Phys 81*:2047-2052.

Tirado MM, Garcia de la Torre J. 1979. Translational friction coefficient of rigid, symmetric top macromolecules. Application to circular cylinders. *J Chem Phys 71*:2581-2587.

Tirado MM, Garcia de la Torre J. 1980. Rotational dynamics of rigid, symmetric top macromolecules. Application to circular cylinders. *J Chem Phys 73*:1986-1993.

Garcia de la Torre J, Martinez MCL, Tirado MM. 1984. Dimensions of short, rodlike macromolecules from translational and rotational diffusion coefficients. Study of the gramicidin dimer. *Biopolymers 23*:611-615.

Zimm BH. 1956. Dynamics of polymer molecules in dilute solution: viscoelasticity, flow birefringence and dielectric loss. *J. Chem. Phys. 24*:269-278.